Vol 13 No 11, November 2004
1009-1963/2004/13(11)/1907-06

Chinese Physics

© 2004 Chin. Phys. Soc.
and IOP Publishing Ltd

Discharge characteristics in plasma display cell at high frequency*

Ouyang Ji-Ting(欧阳吉庭)[a)†], Cao Jing(曹 菁)[a)],
Callegari Thierry[b)], and Boeuf Jean-Pierre[b)]

[a)] *Department of Physics, School of Science, Beijing Institute of Technology, Beijing* 100081, *China*

[b)] *CPAT-CNRS, Université Paul Sabatier,* 118 *Route de Narbonne, Toulouse* 31062, *France*

(Received 23 December 2003; revised manuscript received 5 July 2004)

We present the experimental and simulation studies of the glow discharge plasma in a macroscopic AC plasma display panel cell operating at a high frequency. We find that at high frequencies the plasma from the previous pulse has a significant influence on the discharge properties. The xenon excitation efficiency is larger than that at low frequencies. The discharge mode and efficiency at high frequencies have been discussed in this paper.

Keywords: dielectric barrier discharge, plasma display panel, glow discharge plasma, discharge simulation

PACC: 5280, 5265

1. Introduction

Plasma display panel (PDP) technology is one of the most promising technologies for large-sized, wall-hanging, flat television display applications. The luminous efficacy of conventional coplanar AC PDPs is still low and an important effort has been devoted to its improvement in the last several years.[1] The standard AC PDP cell used by most manufacturers operates in dielectric barrier discharge (DBD) regime in a three-electrode coplanar configuration, with the gap between the coplanar electrodes on the order of 80μm, the operating gas pressure about 5.3–8×10^4Pa in Xe–Ne or Xe–Ne–He mixture with a xenon percentage between 3% and 10%, and the driving frequency of 50–200kHz. PDP discharges form between the coplanar electrodes during the sustaining state (i.e. when the cell is ON), providing VUV photons (emitted from Xe excitation states) which are converted to red, green, or blue light by phosphors. The luminous efficacy is directly related to VUV photon production and hence the Xe excitation efficiency during the discharge. The low luminous efficacy is partly due to the low discharge efficiency in exciting Xe. The principles of the PDP discharges and the reasons for low luminous efficacy can be found in the review by Boeuf.[1]

Improvement of the efficiency can be achieved by operating in different discharge regimes or by optimizing the electrode configuration. Understanding the physical mechanism in PDP discharge is important and necessary for designing highly efficient PDP-configurations. Computer-based modelling is an efficient way to study the physical process and efficacy of PDP cells.[1−7] Another tool that has proved to be very useful in guiding the design of PDP cells is the macro-cell.[1,8−11] The idea is that the small dimensions of a real PDP cell make a systematic and parametric study of the electrode design difficult and costly. We have shown that, although some of the well-known 'scaling laws' may be violated during the afterglow, the discharge behaviour during the current pulse in the macro-cell is very similar to the discharge in a real cell.[8−10] Since it is during the discharge time that the power is deposited into the gas through excitation and ionization, the macro-cell can provide useful information on the efficiency of power deposition into xenon excitation in a real cell. The use of modelling together with experiments on the macro-cell has proved to be extremely efficient for improving our understanding of the physical properties of the plasma and the parameters controlling the cell performances.[1,8−11]

*Project supported in part by the Scientific Research Foundation for Returned Overseas Chinese Scholars, State Education Ministry of China, (Grant No LXKYJJ200403).

†E-mail: jiting.ouyang@263.net

In this paper, we study the effect of frequency on the discharge in PDP. We use a 'macroscopic' cell, which is about 100 times larger than the real cell and operates at a pressure 100 times smaller. The macro-cell and experimental set-up are described in Section 2. The measured and calculated electrode currents, space and time variations of the light emitted by the discharge, and xenon excitation efficiency for different frequency, are shown in Section 3. The effect of frequency on the discharge evolution is discussed in Section 4.

2. Experimetal set-up and modelling

The macro-cell is a glass vessel with internal dimensions 9cm×3cm × 1 cm (see Fig.1) as described in a previous paper.[10] The 'similar' (100 times smaller) PDP cell would be 900 μm × 300μm ×100μm, which is typical of standard discharge cells for 40 inches PDPs. The electrodes are placed outside the vessel, on the 9cm×3cm face. The thickness of the glass of the two 9cm×3cm plates is 3mm, and its relative permittivity is 8. The glass sides of the vessel between the two plates is polished and, transparent ITO is used as a data electrode so that optical measurements are possible from the front and from the side of the discharge cell. The coplanar electrode dimensions are of 3cm × 3cm with coplanar gap of d=0.8cm and the width of ITO data electrode is 1cm in the experiments.

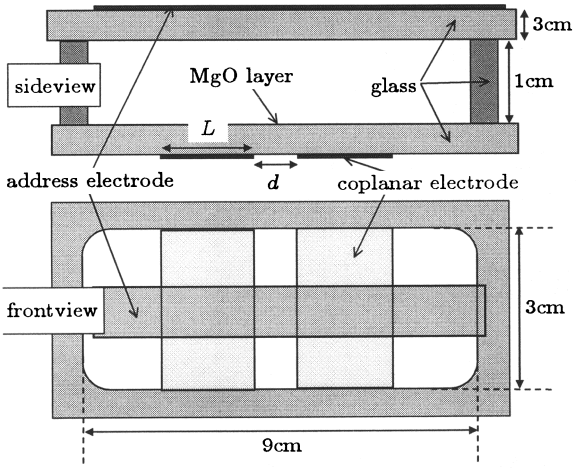


Fig.1. Schematic of the sealed macro-cell. The gas filling is 4% Xe in a Ne–He mixture at 6.6×10^{2}Pa. The electrodes (in ITO or metal) are outside the cell and their position and shape can be easily changed. The coplanar electrode dimensions are 3 cm × 3 cm with a coplanar gap d=0.8cm.

A MgO layer is deposited on the internal sides of the 9cm ×3cm plates by Thomson plasma under well controlled conditions. The cell is evacuated and heated to more than 400°C for several hours, filled with a gas mixture of 4% Xe in Ne–He at 6.6×10^{2}Pa, and sealed.

A square-wave voltage (rise time of the order of 600–700ns) is applied between the two coplanar electrodes, and the address electrode is grounded. The discharge current was measured by using a digital oscilloscope. An intensified CCD camera (ICCD, Princeton Instruments IMAX) with filters (infrared emission around 823 nm or visible emission around 640nm) has been used to measure the time evolution of the xenon and neon emission from the discharge. ICCD images are taken by operating the camera from the front or from the side of the cell.

The simulation results are obtained using the self-consistent two-dimensional (2D) fluid model of the PDP discharge. The 2D model has been described previously.[2,8,9] The gas mixture in the simulation is Xe4%–Ne and the other conditions are the same as those of the macro-cell experiments. The frequency of the sustaining voltage in the simulations is controlled by varying the voltage pulse duration.

3. Results

In this section we first show the specific properties of the discharge evolution at high frequencies, based on experiments and simulations. We then estimate the efficiency of the energy deposition into xenon excitation for different frequencies.

3.1. Discharge current

Figure 2(a) shows the measured currents in the macro-cell for sustaining voltage of V_S=190V at a frequency of f=500 Hz. The applied voltage is set at about 10V above the minimum sustaining voltage for this macroscopic cell. The capacitive current (measured without plasma) associated with the voltage rise time has been subtracted from the total current.

We see in Fig.2 that there are two current pulses on the waveform. The first one is a very short pulse with a duration less than 0.5 μs, starting at the beginning of the applied voltage changing direction. The first pulse is strong, but with an uncertain amplitude in the experiments. It is a discharge between anode and cathode/data electrode. A significant ion current is collected by the data electrode (i.e. acting as a cathode) in this phase and drops to zero very quickly. The second (main) current on the coplanar electrodes begins at time $t \sim 0.5\mu$s. The rising time of the currents

is about 1.8 μs.

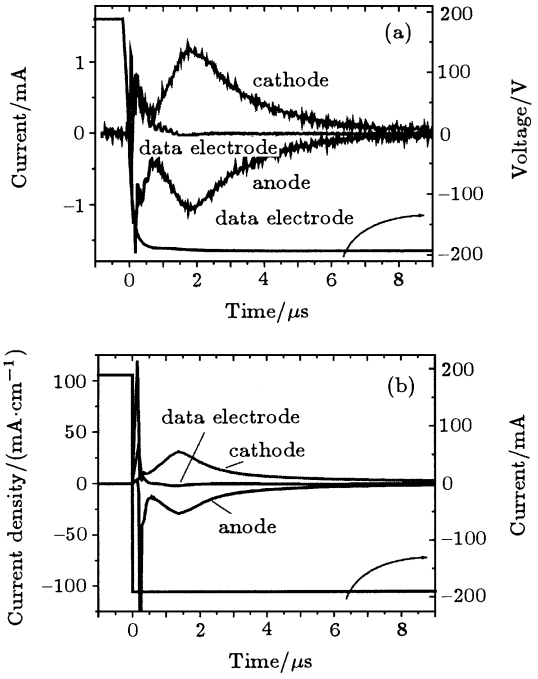


Fig.2. Measured and calculated currents on three electrodes for 190V at 500Hz. (a) Experiment on macro-cell (in Xe4%–Ne–He, 6.6×10^2Pa); (b) simulation on 'similar micro-cell' (in Xe4%–Ne, 6.6×10^4Pa). The time scale of the calculated current has been corrected by using 'similarity laws'.

The experimental currents are in excellent qualitative agreement with the calculated ones from 2D model, as shown in Fig.2(b). The sustaining voltage in the simulation is step-rising pulse, with a duration of τ= 0.5μs. The time scale of the calculated current in Fig.2(b) has been corrected according to the scaling law. We see in Fig.2(b) that there also exists a very short but strong pulse when the voltage changing its direction, similar to the experimental one. Note that in the standard case (short coplanar gap, low frequency), the address electrode does not collect any significant current during sustaining and does not play a fundamental role in the discharge evolution.[8,9] Figure 2 shows that at high frequencies the address electrode plays a specific role in the initial discharge.

3.2. Light emission

We made the images of the infrared emission around 823nm and visible emission around 640 nm from the discharge by using infrared and visible filters, respectively. The two important infrared lines of Xe, at 823 and 828 nm, correspond to the decay of the upper excitation state of xenon to resonance and metastable states Xe($^3P_1$) at 8.31eV and Xe($^3P_2$) at 8.44eV. The decay is fast ($\sim$ 30ns) and it therefore can be used to follow the energy deposited into xenon. The visible emission at 640nm from Ne corresponds to the transition of the $2p^9$ state to $1s^5$ state at 16.62eV. The decay of $2p^9$ is also fast ($\sim$ 20ns) and gives a good image of electron impact excitation of neon.[9] The measurement of infrared and visible lines can also give the information of electron energy distribution of neon excitation which is only expected at electron energy above 16.62eV, while xenon excitation is possible at above 8.31eV.

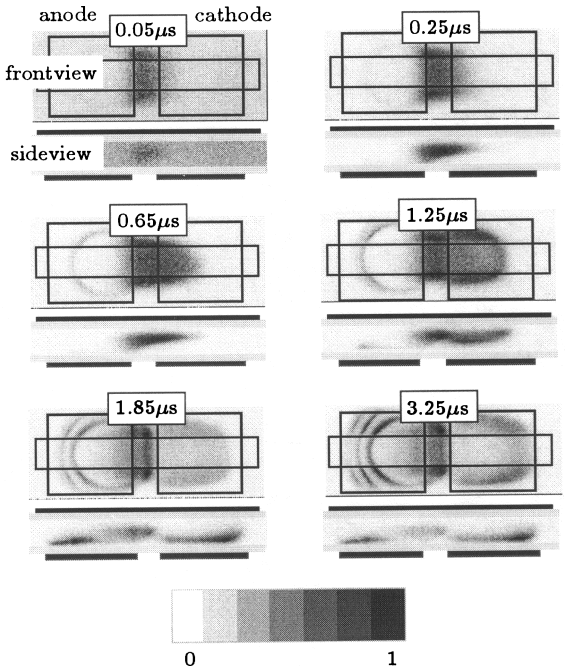


Fig.3. Front view and side view of the space and time variations of xenon infrared emission obtained with the ICCD camera (under the conditions of Fig.2(a)).

Figure 3 shows the time-resolved infrared emission around 823nm (under the condition of Fig.2(a)). The emission intensity has been normalized one by one. Different from that at low frequency where the discharge glow starts above the inner side of the anode after a time lag,[9] the discharge at high frequency initiates in the gap centre at time $t \sim 0$. The plasma fills the central volume of the cell very quickly ($\sim 0.2\mu$s), and develops very fast in two directions, outwards on the anode and cathode. The infrared emission from the glow reaches a maximum in the gap centre at time $t \sim 1.8\mu$s when the current reaches its peak. Then the emission becomes weaker but the centre continues to extend outwards slowly until reaching the outer edge of cathode. The average velocity of the plasma spreading over the cathode (i.e. sheath constriction speed) is about 1.0cm/μs, much faster than at low frequencies

(e.g. ~ 0.3cm/μs for 190V/50Hz in experiments). Stationary striations are observed above the anode during the plasma spreading, as that at low frequencies,[9] but the shape of the striations is distorted to curved lines. The striations may be related to the spatial relaxation of electron energy during the plasma spreading on the dielectric surface above the anode.[9,10]

The plasma spreading over the dielectric surfaces is qualitatively similar to the predictions of the 2D fluid model. The side view of the infrared emission from the plasma can be directly compared to the simulated power deposition into xenon excitation, as shown in Fig.4. The simulation conditions are the same as in Fig.2(b). In Fig.4, the model also shows that the discharge starts in the gap centre at the time of the voltage turn-off. The shapes of the plasma column are similar in experiment and simulation.

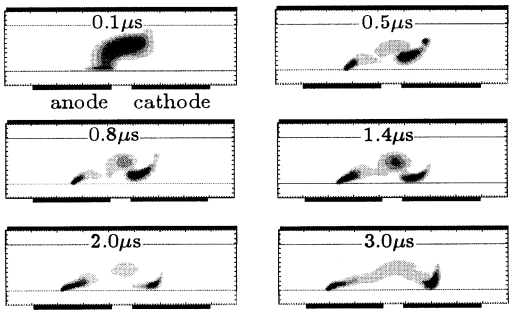


Fig.4. Calculated power deposited in xenon excitation by 2D simulation (under the conditions of Fig.2(b)).

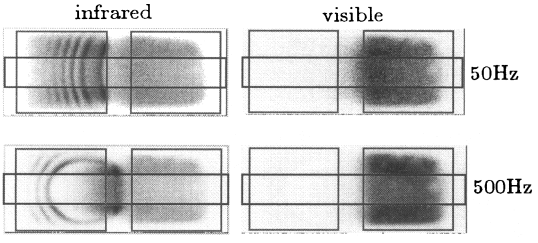


Fig.5. Images of time-integrated infrared and visible emission obtained with the ICCD camera the from front of the macro-cell at 50 and 500Hz.

Figure 5 shows the time-integrated images of infrared and visible emission at f=50 and 500Hz. One can see that the infrared light emission is much stronger at the centre of the coplanar gap at 500Hz, while it is more uniform for 50Hz. This means that the infrared emission centre shifts to the gap centre at a higher frequency. The shape of the infrared emission has distorted. These phenomena have also been seen in the previous experiments.[12] We also found in the experiments that more infrared emission comes from the central region as the voltage increases. The visible emission, however, does not change too much as the frequency increases. It is very weak at the gap centre and practically does not exist above the cathode. Since the infrared emission indicates the lower electron energy hence the lower electric field while the visible emission indicates the higher field region, we can expect that the region of gap centre be a low-field zone and more efficient for electron impact excitation of xenon.

3.3. Discharge efficiency

The VUV photon production and transport in the macro-cell do not follow the similarity laws and we have not tried to measure the VUV emission to characterize the discharge efficiency in producing VUV photons. However, we know that the VUV efficiency is directly related to the efficiency of electron energy deposition in xenon excitation. A large part of this energy contributes to VUV emission.[1] On the other hand, practically most of the xenon excitation occur during the current pulse and, as stated above, the discharge properties during the current pulse are expected to follow the 'similarity laws'. The generation of xenon excited states in the afterglow due to electron–ion recombination is possible in a real high-pressure cell, but this is significant only for current and plasma density larger than those observed under the standard PDP conditions.[8,9]

The efficiency of energy deposition into xenon excitation can be defined as the ratio (η_{Xe}) of the energy spent into electron impact excitation of xenon to the total electric energy dissipated during a discharge pulse. η_{Xe} cannot be measured experimentally, but a quantity which is expected to behave similarly to η_{Xe} can be defined and measured. As we did in a previous paper,[10] we define a 'relative infrared emission efficiency' ρ_{exp} as the ratio of the xenon infrared emissions around 823nm to the neon visible emission around 640nm during one current pulse:

$$\rho_{\mathrm{exp}} = A\frac{\text{IR Xe emission}(\sim 823\text{nm})}{\text{visible Ne emission }(\sim 640\text{nm})}$$

where the infrared and visible emission (around 823 and 640nm, respectively) are integrated in space and time over one current pulse. A is an arbitrary constant which can be adjusted for comparisons with model results, or ratio ρ_{model} of energy deposited in Xe upper excitation (corresponding to the states above the

resonant and metastable states of Xe) to Ne excitation. The value is set to be 0.62 in this paper. Since the infrared emission of xenon is related to the energy deposited into xenon excitation, and the visible emission of neon is related to the energy deposited in the sheath (which is a large part of the total energy deposited in the discharge), one can expect that the ratio $\rho_{\rm exp}$ will roughly resemble the variation of the discharge efficiency in exciting xenon $\eta_{\rm Xe}$, when the discharge parameters are changed. It can therefore be said that the xenon excitation efficiency $\eta_{\rm Xe}$ increases monotonically with $\rho_{\rm exp}$ and can be used to compare the relative efficiency of different configurations.[10]

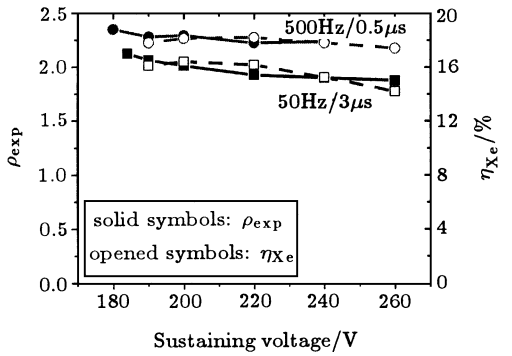


Fig.6. The measured ratio of infrared emission to visible emission $\rho_{\rm exp}$, and the calculated xenon excitation efficiency $\eta_{\rm model}$ as a function of sustaining voltage at different frequencies.

Figure 6 shows the measured ratio $\rho_{\rm exp}$ of infrared emission from Xe to visible emission from Ne and the calculated xenon excitation efficiency $\eta_{\rm Xe}$ as a function of the sustaining voltage. The ICCD images were integrated in time and space from the front of the macro-cell. Figure 6 also shows that with the increase of the frequency (i.e. from f= 50 to 500Hz in experiment or from τ=3 to 0.5μs in simulation), the discharge efficiency increases. Generally, the efficiency decreases slightly with the increase of sustaining voltage.

4. Discussion

In PDP cell, the transient plasma forms during the glow discharge, then decays during afterglow by recombination, three-body collision or diffusion. The decay time of the plasma (i.e. afterglow duration) depends on the plasma density and the cell structure. If the decay time is much shorter than the cycle of the driving voltage, i.e. the driving frequency is low enough, the plasma from the previous discharge pulse has completely decayed when a new pulse is applied, the discharge is starting from the inner side of anode after a time lag of voltage applying and then develops towards two directions.[3,9] The frequency must however be large enough to ensure that a sufficient number of seed electrons are present at the beginning of a new pulse to prevent current jitter.

For frequencies above a critical value (i.e. at high frequencies), the decay time of the plasma is longer than the cycle of the sustaining voltage. The plasma will still be present at the end of the voltage pulse. Figure 7 shows the calculated number density of ions and electrons at the end of the pulse (under the conditions of Fig.2(b)). One can see that the plasma density is high in the cell volume, with electron/ion density of $10^{11}-10^{13}/{\rm cm}^3$. The central density is located in the gap centre with a value about half of that at the moment of the current peak emergence, which is about 5 $\times 10^{13}/{\rm cm}^3$ in maximum according to the calculation. The main positive ions are Xe^+, whose density is 20 times that of Ne^+, and the Ne^+ ions are concentrated mainly at above the inner side of the cathode.

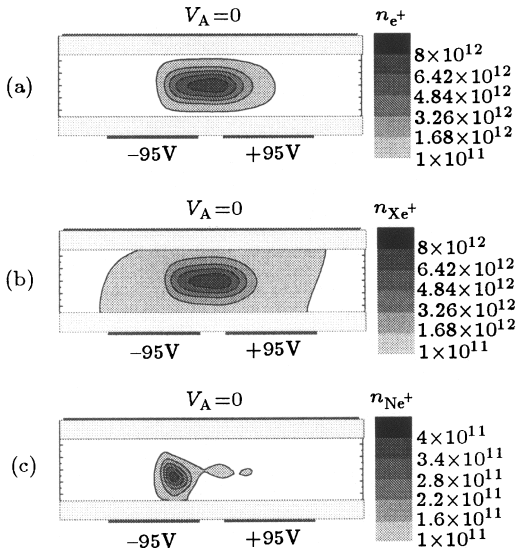


Fig.7. Calculated plasma density distribution at the end of voltage pulse (under the conditions of Fig.2(b)). Figures 7(a)–7(c) are the density distribution for electrons, Xe^+ and Ne^+, respectively. The unit of the number density is $1/{\rm cm}^3$.

We use the influence of frequency on the discharge properties as an estimation of the plasma decay time. According to the experiments and calculations, the decay time is about 3–4ms at 6.6×10^2Pa and $\sim$0.7μs at 6.6×10^4Pa for the present configuration. Note that the 'similarity laws' are violated during the afterglow of PDP discharge because of the electron-ion recombination and three-body collisions, which are important in Xe–Ne mixtures. The afterglow duration in the macro-cell at low pressures is much longer than predicted by the similarity laws. Therefore, a frequency

of 500Hz in the macro-cell in experiments corresponds to a frequency that is much larger than 500Hz × 100=50kHz in the real cell, about 1MHz.

Because there exists the high-density plasma in the cell volume, the accumulated charges on the surface (wall charge) may induce an electric field strong enough to re-ignite the plasma at the instance of pulse turn-off, even if at lower sustaining voltage. Consequently, a self-erase discharge above the electrodes occurs. It is clear in the simulation that a part of positive wall charges above the anode decay very rapidly during this phase. At the same time, some ions are collected by the data electrode. This corresponds the initial current pulse observed in Figs.2 and 3. However, the self-erase discharge will not occur at low frequencies.

Another effect of these high-density charges is that the electric field is distorted significantly. The electron ionization and excitation in the volume is stronger and the plasma develops more quickly. One can therefore expect that the plasma spreading velocity above the cathode is larger than that at low frequencies. At the same time, the electric field near the gap centre is relatively lower because of the space charges. Consequently, the electron energy is lower, and more xenon and less neon molecules can be excited by electron impact. This results in a stronger infrared emission in the central region, as shown in Fig.5.

As is known, a low field is much more efficient for xenon excitation than a high field.[1] Therefore, the positive column is more efficient for infrared emission and VUV generation than the cathode region of a glow discharge. Increasing the length of positive column will improve the discharge efficiency. As mentioned above, at a high frequency the field near the gap centre is lower and much infrared emission comes from that region. This is equivalent to enlarge the positive column. Therefore, the discharge efficiency is expected to be higher at larger frequencies.

On the other hand, the distorted electric field makes the field lines above the anode curved. The plasma spreads above the anode not straightly outwards, but in a radial way to the outer edges of the anode. The shape of the positive column is curved. Therefore, the light striations accompanying the plasma spreading on the dielectric surface are also curved.

5. Conclusion

We have investigated the discharge characteristics at high frequencies in PDP by using macro-cell experiments and 2D fluid simulations. The results show that at high frequencies, a high-density plasma remains in the cell volume at the end of the voltage pulse and has a significant influence on the discharge properties. The decay time of the plasma is about 3–4ms at 6.6×10^2Pa and $\sim 0.7\mu$s at 6.6×10^4Pa for the present configuration. A self-erase discharge occurs at the instance of the voltage changing direction at a high frequency. The infrared emission centre shifts to the region of the gap centre where the electric field is lower. The experiments and simulations show that the discharge is more efficient for xenon excitation and VUV production at higher frequencies, and the discharge efficiency decreases slightly with the increase of the sustaining voltage. The electric field along the dielectric surface in the gap centre and above the anode is distorted and the plasma spreads to the outer sides in a radial way above the anode surface. The light striations are distorted into curved lines consequently.

Acknowledgements

This work was partly supported by Thomson Plasma, France.

References

[1] Boeuf J P 2003 *J. Phys.* D: *Appl. Phys.* **36** R53
[2] Punset C, Boeuf J P and Pitchford L C 1998 *J. Appl. Phys.* **83** 1884
[3] Punset C, Cany S and Boeuf J P 1999 *J. Appl. Phys.* **86** 124
[4] Rauf S and Kushner M J 1999 *J. Appl. Phys.* **85** 3460
[5] Hagelaar G J M, Klein M H, Snijkers R J M and Kroesen G M W 2001 *J. Appl. Phys.* **89** 2033
[6] Seo J H, Chung W J, Yoon C K, Kim J K and Whang K W 2001 *IEEE Trans. Plasma Sci.* **29** 824
[7] Veronis G and Inan U S 2002 *J. Appl. Phys.* **91** 9502
[8] Callegari Th, Ganter R and Boeuf J P 2000 *J. Appl. Phys.* **88** 3905
[9] Ganter R, Ouyang J, Callegari Th and Boeuf J P 2002 *J. Appl. Phys.* **91** 992
Ganter R, Ouyang J, Callegari Th and Boeuf J P 2002 *J. Appl. Phys.* **91** 1000
[10] Ouyang J, Callegari Th, Caillier B and Boeuf J P 2003 *IEEE Trans. Plasma Sci.* **31** 422
[11] Tessier L, Lacoste A, Doyeux H *et al* 2003 *J. Soc. Inform. Display* **11** 551
[12] Ouyang J, Ganter R, Callegari Th and Boeuf J P 2002 *IEEE Trans. Plasma Sci.* **30** 186